REVISTA MATÉRIA V.24 N.01
ISSN 1517-7076 artigo e-12284, 2019

Determination of Barreling of Aluminum Solid Cylinders During Cold Upsetting Using Genetic Algorithm

Erdogan Kanca[1], Omer Eyercioglu[2], Ali Gunen[3], Mehmet Demir[1]

[1] Mechanical Engineering, Engineering and Natural Science Faculty, İskenderun Technical University, 31200, Hatay, Hatay, Turkey
[2] Mechanical Engineering, Engineering Faculty Gaziantep University, 27000, Gaziantep, Gaziantep, Turkey.
[3] Metallurgical and Materials Engineering, Engineering and Natural Science Faculty, İskenderun Technical University, 31200 Hatay, Hatay, Turkey.
e-mail: erdogan.kanca@iste.edu.tr; Mehmet.demir@iste.edu.tr, ali.gunen@iste.edu.tr, omer.eyercioglu@gantep.edu.tr

ABSTRACT

This study presents Genetic Programming models for the formulation of barreling of aluminum solid cylinders during cold upsetting based on experimental results. The maximum and minimum radii of the barreled cylinders having different aspect ratio (d/h= 0.5, 1.0 and 2.0) were measured for various frictional conditions (m=0.1-0.4). The change in radii with respect to height reduction showed different trends before and after folding, therefore, the corresponding reduction ratios of folding were also determined by using incremental upsetting. Genetic programming models were prepared using the experimental results with the input variables of the aspect ratio, the friction coefficient, and the reduction in height. The minimum and maximum barreling radii were formulated as output taking the folding into consideration. The performance of proposed GP models are quite satisfactory (R^2 = 0.908-0.998).

Keywords: Upset, forging, barreling, bulging, axisymmetric compression.

1. INTRODUCTION

Deformation modes of bulk forming processes are mainly upsetting, extrusion or both. Due to its versatility in metal forming applications, upsetting has been considered as an important subject of many researches. In upsetting of a cylinder, the existence of friction between the die and workpiece interface causes non-homogeneous deformation. The interface friction opposes the free expansion of the end faces with two consequences: formation of barreling and friction hill. While barreling changes the deformation patterns, and so the magnitudes of the strain components, friction hill increases the interface pressure to a value higher than the flow stress of the material.

Kulkarni and Kalpakjian [1] have carried out a series of tests in which specimens were upset in different lubrication conditions and they examined the shape of the barrel. A comprehensive literature review has been published by Johnson and Mellor [2]. Avitzur [3] has developed an upper bound solution for disc forging. An incremental elasto-plastic finite element method has been used to study the influence of the friction on the deformation of solid cylinders [4]. Schey et al [5] conducted upsetting tests to evaluate the factors that affect the shape of the barrel. The upset forging of cylindrical billets having unequal interfacial friction conditions have been studied by different workers [6-8]. Folding has also been treated in many studies [3,8]. Saluja et al [9] suggested a method for flow stress determination introducing a bulge correction factor which depends on maximum and minimum radii of the compressed cylinder.

In recent studies [10-11], barreling phenomenon was investigated experimentally at various friction and geometrical conditions. The radius of curvature of the barrel was expressed as a function of height reduction depending on the maximum and minimum radii of the billet which can only be obtained by measuring compressed cylinder.

Estimation of the amount of barreling beforehand is of great importance for industrial applications as it facilitates the determination of the appropriate die design and the press capacity needed to design the respective die. Therefore, this study focused on present a mathematical formulation for determination of barreling (minimum and maximum radii) of solid aluminum cylinders during cold upsetting. For this purpose, a

Corresponding Author: Ali Gunen Received on: 27/03/2017 Accepted on: 23/02/2018

10.1590/S1517-707620190001.0621

series of billets having different aspect ratio were cold upset with various friction conditions. A genetic programming model for the formulation is prepared using the experimentally predicted data.

2. MATERIALS AND METHODS

2.1 Material

Cylindrical billets of 20 mm in diameter and different heights corresponding to a set of aspect ratio (d/h=0.5, 1.0, 2.0) were prepared by machining from 30 mm rods of annealed aluminum 1100 (99.42 wt% Al, 0.111 wt% Si, 0.066 wt% Mn, 0.333 wt% Fe, 0.014 wt% Cr, 0.031 wt% other) were used as the billets. The billets were upset at room temperature on a hydraulic press having 600 kN capacity. Top and bottom platens were prepared from AISI 4340 steel and their working surfaces were hardened and ground. To obtain the proper deformation pattern, care was taken to perpendicularity and concentricity between platens and the billets. The schematic views of strains and billet are illustrated in Figures 1 and 2, respectively.

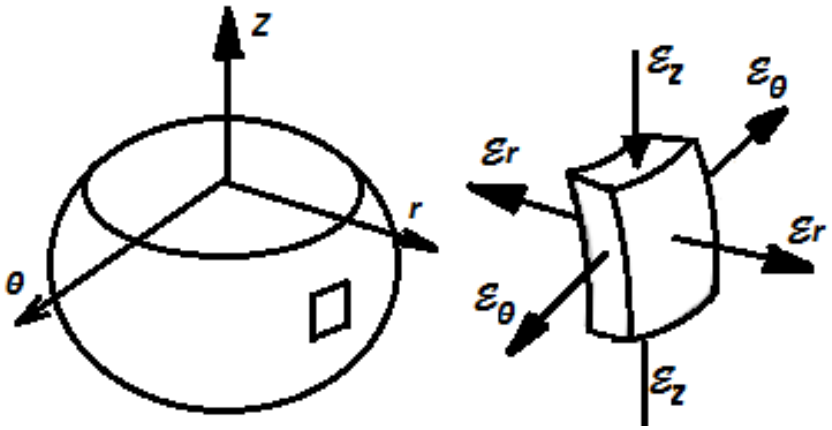

Figure 1: Schematic view of strains after deformation

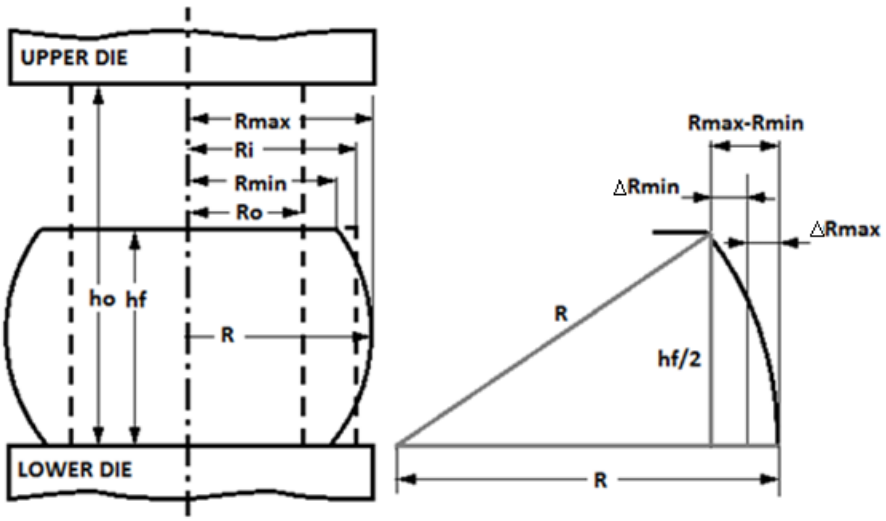

Figure 2: Schematic view of billet before and after deformation.

Ring compression tests were carried out to determine the friction factor (m) for dry and various lubricating conditions. The rings were produced from the same material of the upsetting billets (annealed

aluminum 1100) with a ratio of 6:2:1 (OD:ID:H). The surfaces of the die platens were purposely textured with respect to various lubricants to obtain proper friction factors. The friction factors were determined from the chart presented by Lahoti G. D., et al [12]. The lubrication condition and the determined friction factors are given in Table 1.

Table 1: Type of lubrication and corresponding friction factor

Lubrication	Friction factor (m)
Palm oil	0.1
MoS_2	0.2
Graphite	0.3
Dry	0.4

The heights, minimum and maximum radii of the billets were measured using a digital micrometer and the radius of curvature of the barrel was measured using a 3-D Coordinate Measuring Machine (CMM).

2.2 Method

The main focus of this study is to obtain three genetic programming models for the formulations of the minimum and maximum radii of cylindrical aluminum billets and their folding point (i.e., where a part of the initially free surface comes into contact with the die during upset forging) during cold upsetting based on experimental results. For this purpose, genetic programing was used to prepare mathematical model in the barreling processes.

Genetic programming is an extension of genetic algorithms, first introduced by Koza [13] to be able to get automatically intelligible relationships in a system. It has been used successfully in many applications and areas [14,15]. While GA uses a string of numbers to represent the solution, GP automatically generates several computer programs (CP) with a sorting table to solve the problem considered [13]. The GP generates a population of computer programs with a sorting tree structure. Randomly generated programs, in terms of size and structure, are generic and hierarchic. GP's main goal is to solve a problem by searching optimal computer programs in the space of all possible solutions. Thus, it allows to achieve the optimum results [16].

Gene Expression Programming (GEP) software, used in this study, is an extension of GP. It evolves computer programs of different sizes and shapes encoded in linear chromosomes of fixed length and it was introduced by Candida Ferreira [17]. Multiple genes, each gene encoding a smaller sub-programs, are created by chromosomes. Furthermore, the structural and functional organization of the linear chromosomes allows the unconstrained operation of important genetic operators such as mutation, transposition, and recombination. One of the strong points of the GEP approach is that the generation of genetic diversity is extremely simplified as genetic operators work at the chromosome level. In addition thanks to the multigenic nature it allows to the evolution of more complex programs. As a result of this, GEP exceeds, 100-1000 fold, the former GP system [17]. GEP was used in this study due to its unique properties. The fundamental difference between Genetic Algorithm (GA), GP and GEP is due to the nature of the individuals: in GAs the individuals are linear strings of fixed length (chromosomes); in GP the individuals are nonlinear entities of different sizes and shapes (parse trees); and in GEP the individuals are encoded as linear strings of fixed length which are afterwards expressed as nonlinear entities of different sizes and shapes. Therefore, the distinguishing parameters of GEP are chromosomes and expression trees (ETS). Translation, analysis of information from the chromosomes to the ETS, is depend on a specific set of rules. The genetic code is very simple where there exist one-to-one relationships between the symbols of the chromosome and the functions or terminals they represent. Spatial organization and terminals in the ETs and type of interaction between sub-ETs can be determined easily by rules [17,18]. That's why two languages are used in the GEP: the language of the genes and the language of ETs. A significant advantage of GEP is that it enables us to infer exactly the phenotype given the sequence of a gene, and vice versa which is termed as Kavra language.

The details of the experimental database including the parameters and ranges of them are presented in Table 2. Parameters of the GEP models are presented in Table 3. The list of function is given in Table 4. Genetic programming models were prepared using the experimental results with the input variables of the aspect ratio, the friction coefficient, and the reduction in height. The minimum and maximum barreling radii

were formulated as output taking the folding into consideration.

Table 2: The variables used in models construction

Model	Code	Input variable	Range	Code	Output variable	Range
Folding	d0	d/h	0.5-2	D.V	hf/h	0.2-0.92
	d1	m	0-0.4			
ΔR_{min}	d0	d/h	0.5-2	D.V	ΔRmin	0.065-4.087
	d1	m	0-0.4			
	d2	hf/h	0.2-0.92			
ΔR_{max}	d0	d/h	0.5-2	D.V	ΔRmax	0.017-0.916
	d1	m	0-0.4			
	d2	hf/h	0.2-0.92			

Table 3: Parameter of the GEP models

P1	Function Set	+, -, *, /, √, ex, ln, log, tan, X^2, X^3
P2	Number of Genes	1,2,3,4,5,6
P3	Head Size	3, 5, 8, 10, 12, 15
P4	Linking Function	Addition (+), Multiplication (*)
P5	Number of Generation	10000 and 20000
P6	Chromosomes	30-45
P7	Mutation Rate	0.044
P8	Inversion Rate	0.1
P9	One-point Recombination Rate	0.3
P10	Two-point Recombination Rate	0.1
P11	Gene Recombination Rate	0.1
P12	Gene transposition Rate	0,1

Table 4: List of function sets

Code	Function Set
S1	+, -, *, /
S2	+, -, *, /, √
S3	+, -, *, /, √, e^x
S4	+, -, *, /,√, ln
S5	+, -, *, /, √, e^x, X^2, X^3
S6	+, -, *, /, √, e^x, ln, X^2, X^3

3. RESULTS AND DISCUSSIONS

3.1 Experimental results

Although unidirectional movement of the die (top die was descending while bottom die was stationary) was applied, radii of top and bottom surfaces of the billets are almost same because of the equal interface frictional conditions and the lower speed of compression. A symmetrical deformation from top to bottom was observed on the billets, so that, top surface radii (R_{min}) and barreling radii of the billets (R_{max}) were measured.

Strain paths at the barreling surface are shown in Figures 3 and 4 with respect to aspect ratio and friction factor. As expected, amount of barreling and hoop strain are increasing with friction factor [19]. The aspect ratio has a similar effect, however, the difference between d/h=1 and 2 is much smaller than d/h=0.5.

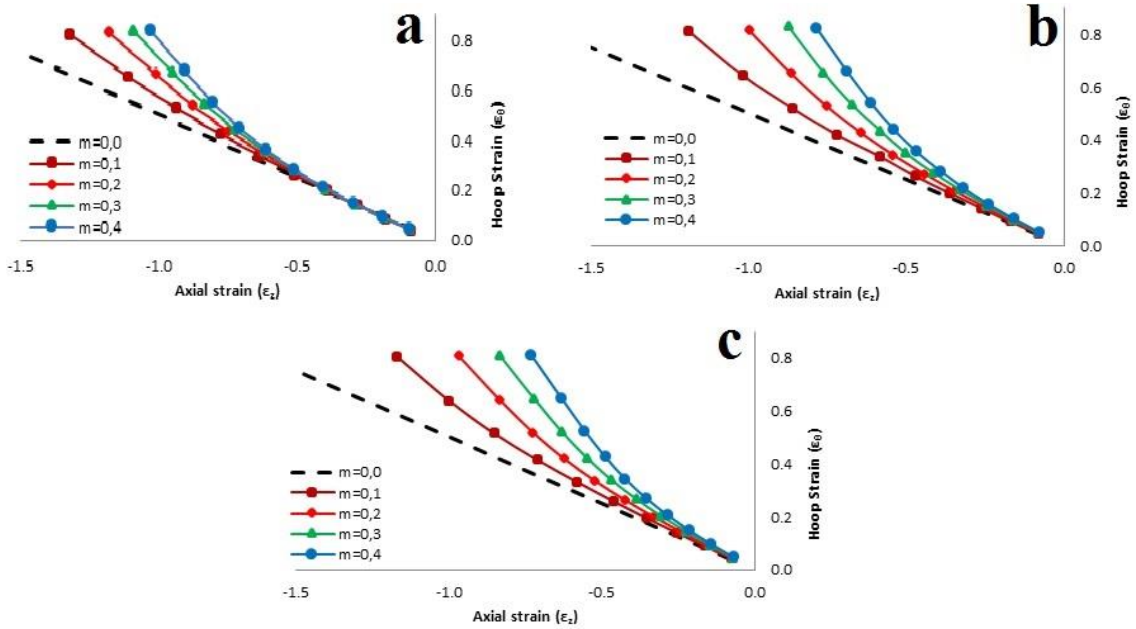

Figure 3: Strain path at the barreling surface with respect to aspect ratio, (a) d/h=0.5, (b) d/h=1.0, (c) d/h=2.0

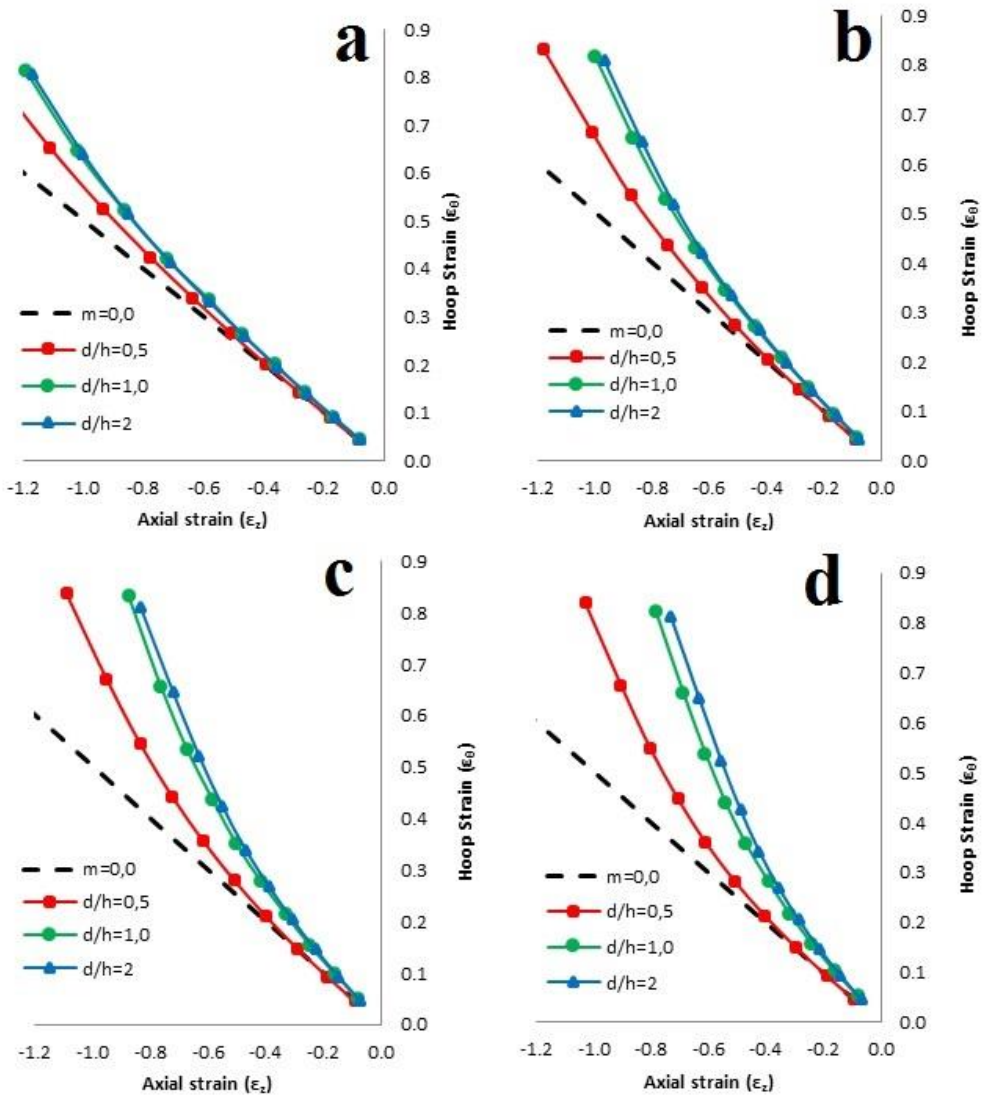

Figure 4: Strain path at the barreling surface with respect to. friction factor, m=0.1, (b) m=0.2, (c) m=0.3, (d) m=0.4.

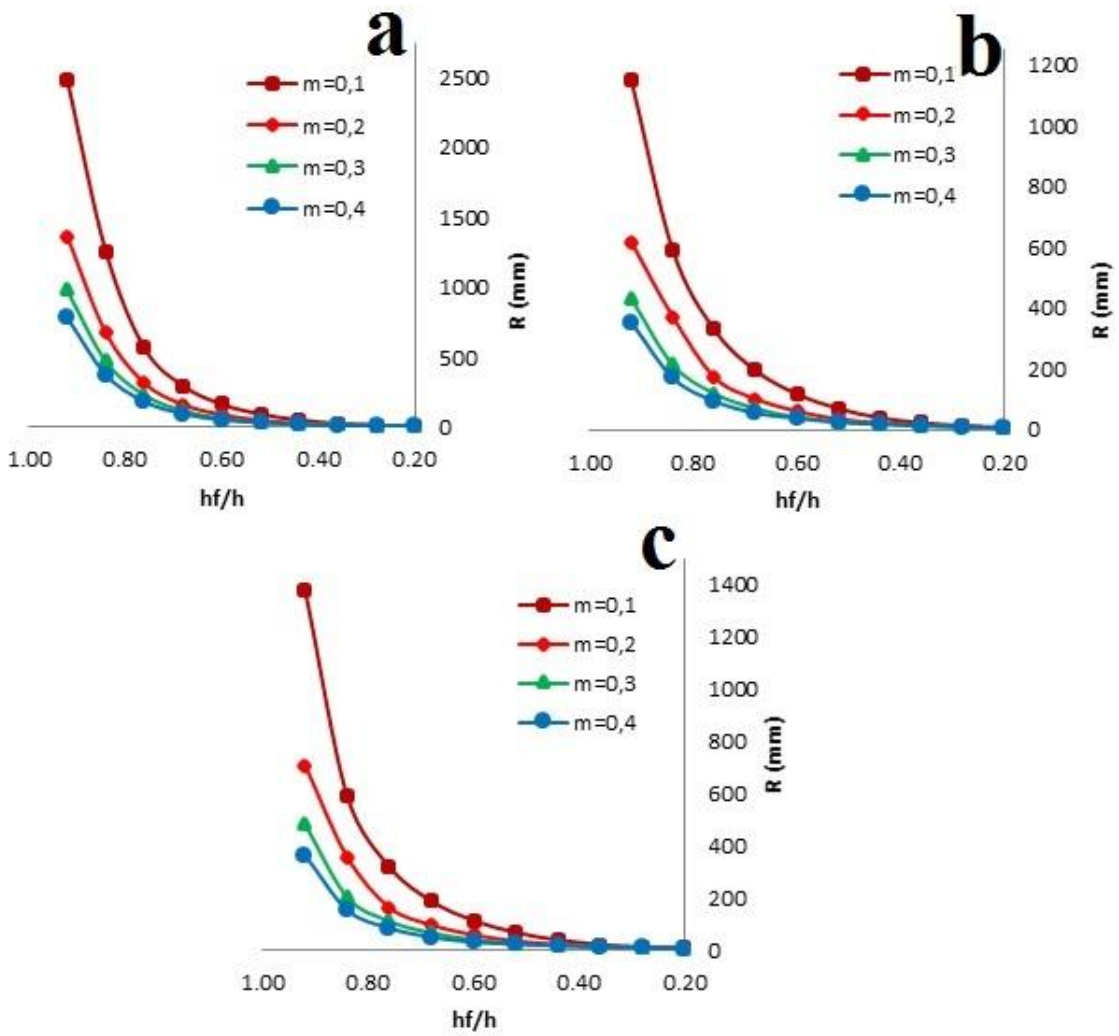

Figure 5: The radius of curvatures of the barreling against reduction in height (h_f/h); d/h=0.5, (b) d/h=1 and (c) d/h=2

The radius of curvatures of the barreling obtained from the 3-D CMM measurements are plotted against reduction in height (h_f/h) in Figure 5. Obviously, increasing amount of bulging reduces curvature dramatically.

The deviation of R_{min} and R_{max} from the corresponding radii of homogeneous deformation (R_i) were determined and plotted with respect to reduction in height (h_f/h) as shown in Figure 6. Both ΔR_{min} and ΔR_{max} values are increasing with increasing friction factor [20].

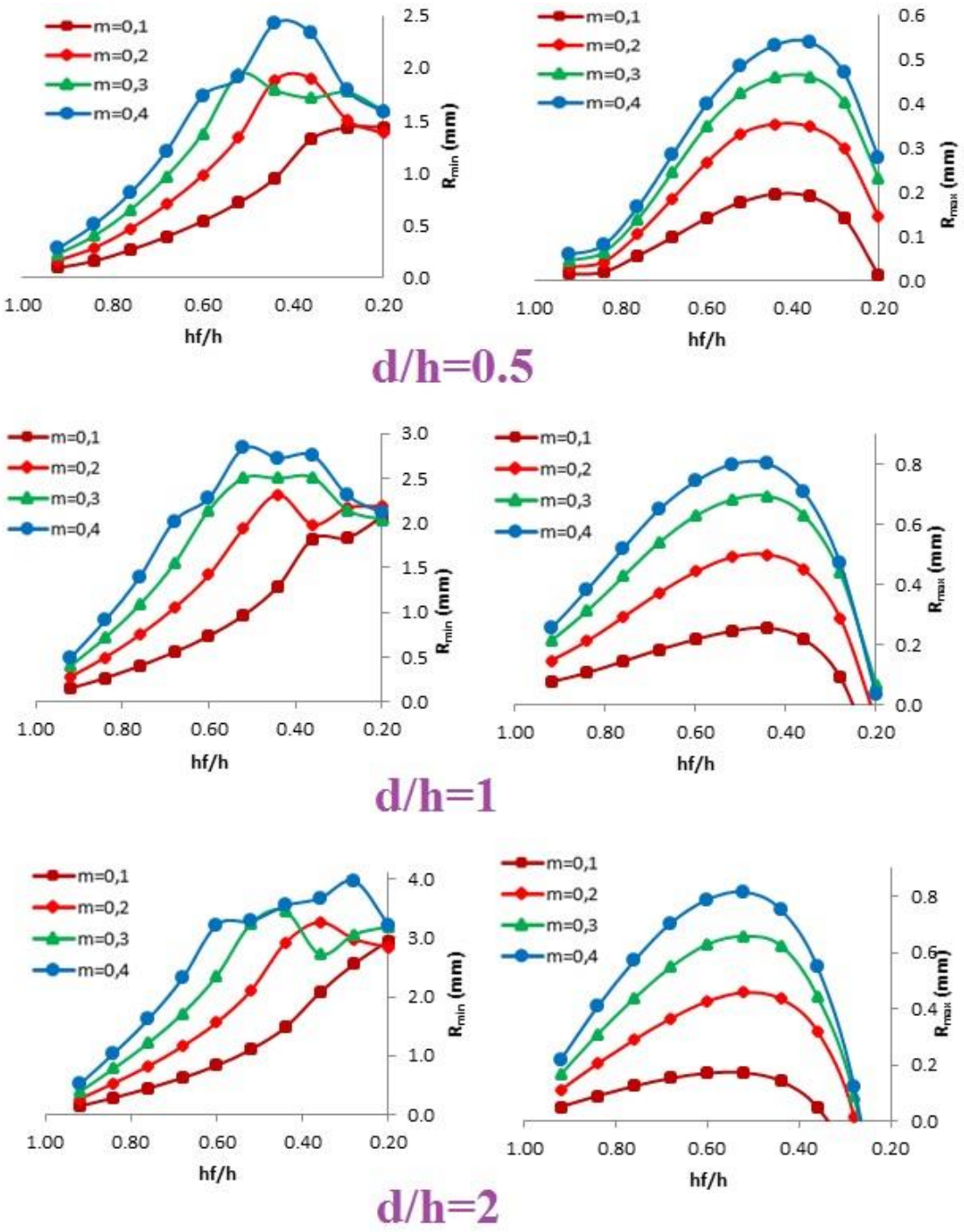

Figure 6: The deviation of R_{min} and R_{max} from the corresponding radii of homogeneous deformation (R_i) were determined and plotted with respect to reduction in height (h_f/h) for d/h=0.5; (a) R_{min} and (b) R_{max}

The trend of ΔR_{max} is very similar for different aspect ratios and they have a maximum at a specific (h_f/h) value. However, ΔR_{min} curves are uneven after some values of (h_f/h). This is due to folding where a part of the initially free surface comes into contact with the die.

In figure 7, corresponding (h_f/h) values of folding for various friction and aspect ratio are given. It can be seen from the figure, rate of hf/h increased with the increase the friction coefficient and increasing in the rate of d/h caused to decrease in the hf/h rate in all experiments conditions.

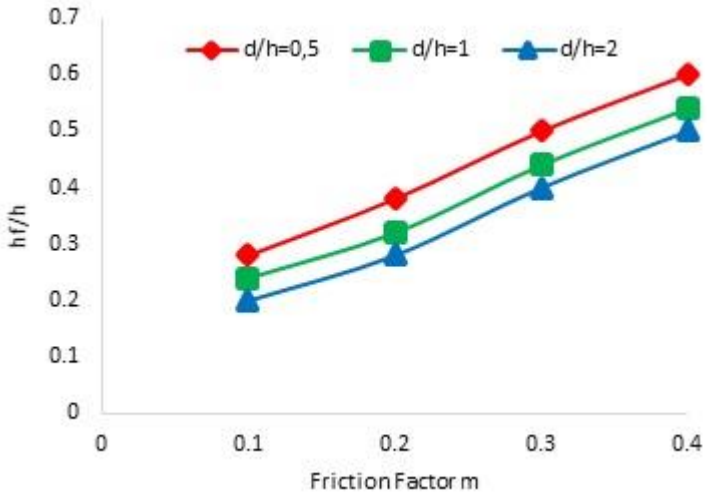

Figure 7: Corresponding (h_f/h) values of folding for various friction and aspect ratio.

3.2 Results of numerical application and GEP formulations

Three genetic programming models were used for the formulations of the minimum and maximum barreling radii of billets and their folding point during cold upset forging. All tried combinations obtained from the GEP results are presented in Table 5 for folding point, in Table 6 for ΔRmin and in Table 7 for ΔRmax, respectively.

Table 5: The best and the worst results obtained from the GEP tests for folding point

P2	P3	P4			R^2 Error				R^2 Error	
			P1	P5	Training	Test	P1	P5	Training	Test
1	**7**		**S1**	**12982**	**0.999**	**0.998**	S4	10918	0.978	0.967
2	8	+	S1	13876	0.989	0.971	S4	14763	0.989	0.956
2	8	*	S1	17987	0.992	0.991	S4	12835	0.978	0.965
1	7		S2	10982	0.937	0.912	S5	12982	0.919	0.927
2	8	+	S2	19276	0.945	0.938	S5	11022	0.978	0.987
2	8	*	S2	11287	0.992	0.987	S5	12023	0.996	0.991
1	7		S3	10987	0.918	0.901	S6	17934	0.987	0.991
2	8	+	S3	10234	0.902	0.918	S6	12922	0.992	0.990
2	8	*	S3	12897	0.992	0.989	S6	17823	0.987	0.919

Table 6: The best and the worst results obtained from the GEP tests for ΔR_{min}

				R^2 Error					
P1	**P2**	**P3**	**P4**	**Before Folding**			**After Folding**		
				P5	**Training**	**Test**	**P5**	**Training**	**Test**
S1	**1**	**7**		**12789**	**0.972**	**0.961**	11092	0.881	0.941
S1	2	8	+	10987	0.957	0.920	12928	0.925	0.798
S1	2	8	*	10098	0.952	0.966	13098	0.882	0.918
S1	3	10	+	17345	0.946	0.956	12098	0.931	0.752
S1	3	10	*	12674	0.961	0.957	17646	0.927	0.795
S2	1	7		15897	0.868	0.895	13756	0.885	0.948
S2	2	8	+	13980	0.927	0.929	12345	0.902	0.867
S2	2	8	*	12453	0.918	0.891	12876	0.916	0.800
S2	3	10	+	14098	0.927	0.952	14908	0.904	0.890
S2	3	10	*	17908	0.976	0.944	15093	0.925	0.765
S3	1	7		19037	0.874	0.912	10289	0.889	0.930
S3	2	8	+	18905	0.919	0.916	17893	0.931	0.842
S3	2	8	*	17457	0.950	0.962	13098	0.902	0.848
S3	3	10	+	14098	0.953	0.933	14678	0.913	0.853
S3	3	10	*	12098	0.952	0.911	16782	0.916	0.824
S4	**1**	**7**		10982	0.928	0.947	**17829**	**0.929**	**0.910**
S4	2	8	+	11902	0.937	0.885	17294	0.917	0.804
S4	2	8	*	12098	0.969	0.959	19038	0.892	0.905
S4	3	10	+	10928	0.944	0.948	18990	0.936	0.741
S4	3	10	*	11098	0.974	0.945	12782	0.935	0.762
S5	1	7		12346	0.837	0.889	18296	0.888	0.914
S5	2	8	+	11093	0.952	0.953	12983	0.909	0.900
S5	2	8	*	19022	0.951	0.961	13739	0.904	0.857
S5	3	10	+	18902	0.939	0.964	11902	0.948	0.774
S5	3	10	*	19025	0.956	0.965	11386	0.934	0.807
S6	1	7		12987	0.819	0.897	11091	0.890	0.904
S6	2	8	+	11238	0.937	0.938	10982	0.922	0.755
S6	2	8	*	12092	0.974	0.951	18296	0.913	0.879
S6	3	10	+	11092	0.938	0.935	17298	0.930	0.840
S6	3	10	*	19029	0.960	0.961	12987	0.922	0.869

Table 7: The best and the worst results obtained from the GEP tests for ΔR_{max}

				R^2 Error					
P1	**P2**	**P3**	**P4**	**Before Folding**			**After Folding**		
				P5	**Training**	**Test**	**P5**	**Training**	**Test**
S1	1	7		18724	0.735	0.734	19028	0.831	0.727
S1	2	8	+	18414	0.903	0.870	18290	0.887	0.615
S1	2	8	*	10552	0.934	0.916	10234	0.896	0.665
S1	3	10	+	11913	0.961	0.951	11098	0.931	0.813
S1	3	10	*	19366	0.950	0.934	10926	0.899	0.907
S2	1	7		19742	0.795	0.848	10922	0.759	0.543
S2	**2**	**8**	**+**	**17399**	**0.933**	**0.928**	11098	0.868	0.637
S2	2	8	*	15283	0.909	0.904	12456	0.618	0.747
S2	3	10	+	14567	0.905	0.894	18654	0.899	0.824
S2	3	10	*	14154	0.964	0.960	19546	0.898	0.764
S3	1	7		13700	0.744	0.696	17546	0.826	0.474
S3	2	8	+	13717	0.861	0.886	13893	0.895	0.735
S3	2	8	*	17565	0.822	0.825	19296	0.881	0.805
S3	3	10	+	19127	0.815	0.848	10289	0.943	0.873
S3	3	10	*	18178	0.888	0.849	14628	0.908	0.751
S4	1	7		19174	0.689	0.802	18021	0.772	0.703
S4	2	8	+	18216	0.900	0.877	10012	0.901	0.720
S4	2	8	*	15219	0.909	0.906	**19012**	**0.910**	**0.901**
S4	3	10	+	17620	0.918	0.906	19037	0.930	0.861
S4	3	10	*	17720	0.907	0.887	16345	0.908	0.745
S5	1	7		15404	0.824	0.863	13752	0.735	0.632
S5	2	8	+	19789	0.888	0.882	12903	0.844	0.561
S5	2	8	*	17591	0.893	0.878	19820	0.904	0.861
S5	3	10	+	18601	0.946	0.925	12903	0.904	0.881
S5	3	10	*	19603	0.959	0.974	11098	0.940	0.838
S6	1	7		18655	0.774	0.799	10283	0.737	0.815
S6	2	8	+	17264	0.894	0.874	11902	0.910	0.816
S6	2	8	*	18033	0.907	0.917	16830	8.892	0.844
S6	3	10	+	18858	0.942	0.922	18936	0.904	0.759
S6	3	10	*	17536	0.934	0.951	12903	0.874	0.922

There are many different combinations of the GEP parameters, which mean as lots of GEP models. Running the GEP algorithm for all of these combinations requires a huge amount of computational time. Therefore, a subset of these combinations is selected intuitively to investigate the performance of the GEP algorithm in predicting the folding point, ΔRmin and ΔRmax. The optimal setting is demonstrated as bold in the tables. Therefore these optimal settings are used for the prediction of the folding point, ΔR_{min} and ΔR_{max}. Table 8 illustrates the training and test evaluation of the GEP method for the folding point prediction. Figure 8-12 show expression trees for folding, ΔR_{min} and ΔR_{max} before and after folding point.

Table 8: Statistical values of best result of GEP formulation.

			ΔR_{min}				ΔR_{max}			
	Folding Point		**Before Folding**		**After Folding**		**Before Folding**		**After Folding**	
	Train	**Test**	**Train**	**Test**	**Train**	**Test**	**Train**	**Test**	**Train**	**Test**
MSE	0,0003	0,0005	0,061	0,045	0,045	0,037	0,003	0,003	0,006	0,008
MAE	0,0160	0,0205	0,172	0,158	0,165	0,172	0,044	0,046	0,071	0,073
R	0,9995	0,9889	0,971	0,980	0,943	0,964	0,966	0,963	0,911	0,902

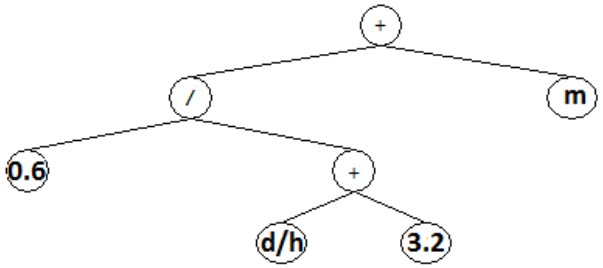

Figure 8: Expression tree for folding.

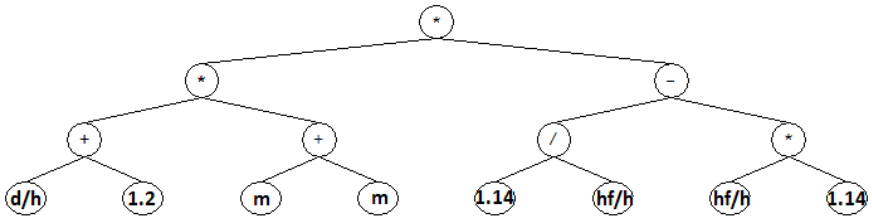

Figure 9: Expression tree for ΔR_{min} before folding.

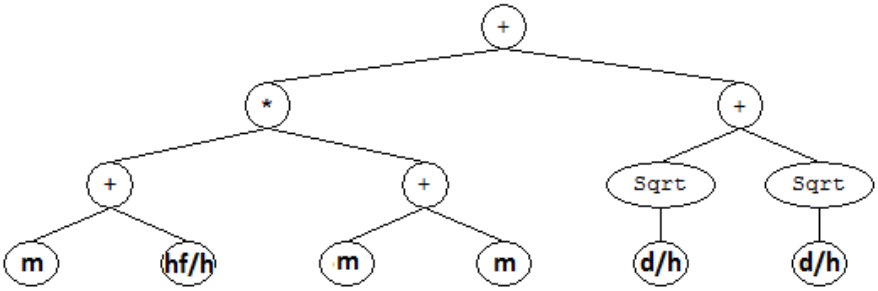

Figure 10: Expression tree for ΔR_{min} after folding.

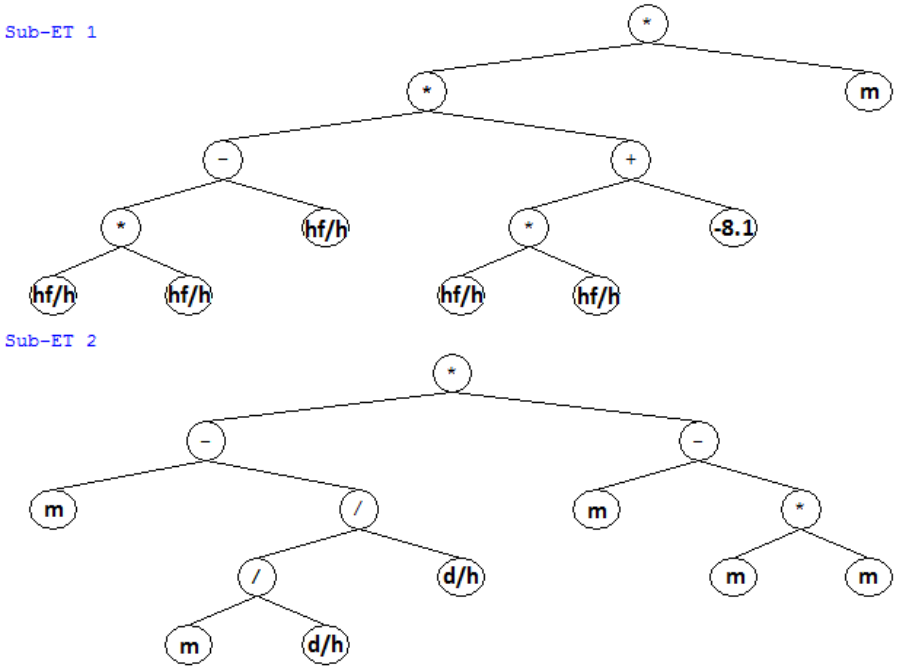

Figure 11: Expression tree for ΔR_{max} before folding.

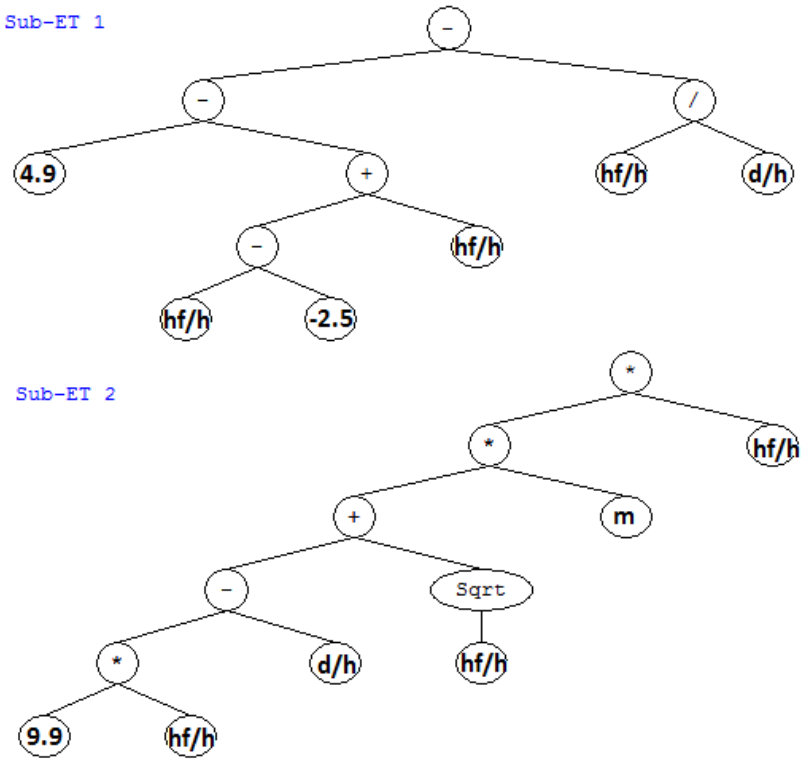

Figure 12: Expression tree for ΔR_{max} after folding.

To achieve generalization capability for the formulations, the experimental database is divided into two sets as training and test sets. The formulations are based on training sets and are further tested by test set values to measure their generalization capability. Statistical parameters of test and training sets of GP formulations are presented in Table 8 where R; MSE and MAE corresponds to the coefficient of correlation, mean square error and the mean absolute error of proposed GEP model, respectively as seen in Table 8. In literature [18, 19], this type of studies includes test sets as 20%–30% of the train set. The patterns used in test and training sets are selected in systematic randomly. Regarding the ΔR_{min} and ΔR_{max} formulation, 90 training and 30 tests were used as training and test sets in Table 9 and Table 10, respectively. It should be noted that the proposed GP formulation is valid for the ranges of training set given in Table 2. Figure 13 and Figure 14 show the training and test evaluation of the GEP method for the R_{min} and R_{max} predictions.

The obtained expression tree of the formulation is shown in Figure 8 – 12 which corresponds to the following equation:

$$\left(\frac{h_f}{h}\right)_{folding} = m + \frac{0.6}{\left[\frac{d}{h}+3.2\right]} \quad (1)$$

$$\Delta Rmin_{Before\ f} = 1.14 * \left[\frac{h}{h_f} - \frac{h_f}{h}\right] * \left[1.2 + 2m + \frac{d}{h}\right] \quad (2)$$

$$\Delta Rmin_{After\ f} = 2 * \sqrt{\frac{d}{h}} + 2 * m * \left[m + \frac{h_f}{h}\right] \quad (3)$$

$$\Delta Rmax_{Before\ f} = m * \left[\left(\frac{h_f}{h}\right)^2 - \left(\frac{h_f}{h}\right)\right] * \left[\left(\frac{h_f}{h}\right)^2 - 8.1\right] + (m + m^2) * \left[m - \frac{m}{\left(\frac{d}{h}\right)^2}\right] \quad (4)$$

$$\Delta Rmax_{After\ f} = m * \frac{h_f}{h} * \left[4.9 - \left(2 * \frac{h_f}{h} + 2.5\right) - \frac{h_f}{h}\right] * \left[9.9 * \frac{h_f}{h} + \sqrt{\frac{h_f - d}{h}}\right] \quad (5)$$

$$Ri = \frac{d}{2 * \sqrt{\frac{h_f}{h}}} \quad (6)$$

$$R_{min}=R_i-\Delta R_{min} \quad (7)$$

$$R_{max}=R_i+\Delta R_{max} \quad (8)$$

From geometry (see figure 2) the radius of curvature of barrel is:

$$R=\frac{h_f^2+2*(R_{max}-R_{min})^2}{8*(R_{max}-R_{min})} \quad (9)$$

Table 9: Results of GP formulation versus training results.

				R_{min}		R_{min}(T/GP)	R_{max}		R_{max}(T/GP)
No:	**m**	**d/h**	**hf/h**	**Test**	**GP**		**Test**	**GP**	
1	0,1	0,5	0,84	13,48	13,50	0,9985	13,66	13,71	0,9961
2	0,1	0,5	0,76	14,08	14,12	0,9967	14,39	14,45	0,9962
3	0,1	0,5	0,68	14,77	14,85	0,9945	15,26	15,30	0,9972
4	0,1	0,5	0,6	15,60	15,72	0,9921	16,28	16,30	0,9989
5	0,1	0,5	0,52	16,62	16,79	0,9898	17,51	17,50	1,0005
6	0,1	0,5	0,44	17,90	18,13	0,9869	19,04	19,01	1,0014
7	0,1	0,5	0,2	26,52	26,49	1,0010	27,96	28,02	0,9981
8	0,2	0,5	0,92	12,87	12,90	0,9975	13,06	13,04	1,0015
9	0,2	0,5	0,76	13,87	13,91	0,9975	14,44	14,52	0,9948
10	0,2	0,5	0,68	14,46	14,55	0,9942	15,34	15,40	0,9966
11	0,2	0,5	0,6	15,16	15,31	0,9901	16,40	16,41	0,9994
12	0,2	0,5	0,52	15,99	16,25	0,9842	17,67	17,63	1,0020
13	0,2	0,5	0,44	16,96	17,43	0,9733	19,20	19,14	1,0031
14	0,2	0,5	0,28	22,12	22,00	1,0053	23,92	23,83	1,0036
15	0,3	0,5	0,92	12,81	12,84	0,9977	13,08	13,00	1,0056
16	0,3	0,5	0,76	13,69	13,69	1,0001	14,48	14,56	0,9942
17	0,3	0,5	0,68	14,19	14,24	0,9966	15,40	15,47	0,9956
18	0,3	0,5	0,6	14,76	14,90	0,9908	16,49	16,51	0,9987
19	0,3	0,5	0,52	15,39	15,70	0,9803	17,76	17,73	1,0013
20	0,3	0,5	0,44	17,06	16,94	1,0067	19,30	19,26	1,0020
21	0,3	0,5	0,28	21,85	21,87	0,9994	24,03	23,94	1,0036
22	0,3	0,5	0,2	26,36	26,27	1,0034	28,18	28,14	1,0014
23	0,4	0,5	0,92	12,76	12,77	0,9986	13,09	12,96	1,0102
24	0,4	0,5	0,84	13,14	13,10	1,0031	13,72	13,75	0,9978
25	0,4	0,5	0,76	13,53	13,48	1,0040	14,50	14,60	0,9934
26	0,4	0,5	0,68	13,95	13,93	1,0011	15,44	15,54	0,9938
27	0,4	0,5	0,52	15,42	15,19	1,0157	17,82	17,76	1,0032
28	0,4	0,5	0,44	16,42	16,76	0,9793	19,38	19,40	0,9986
29	0,4	0,5	0,36	18,50	18,82	0,9831	21,37	21,37	0,9999
30	0,4	0,5	0,2	26,37	26,07	1,0114	28,23	28,21	1,0007
31	0,1	1	0,92	25,91	25,98	0,9973	26,14	26,12	1,0009
32	0,1	1	0,76	28,28	28,40	0,9957	28,82	28,81	1,0003
33	0,1	1	0,68	29,76	29,92	0,9947	30,50	30,48	1,0006
34	0,1	1	0,6	31,54	31,74	0,9936	32,49	32,46	1,0010
35	0,1	1	0,44	36,39	36,77	0,9897	37,95	37,88	1,0016
36	0,1	1	0,36	39,84	40,46	0,9848	41,89	41,85	1,0008
37	0,1	1	0,2	53,83	53,94	0,9980	55,70	55,96	0,9955

38	0,2	1	0,92	25,78	25,90	0,9956	26,21	26,17	1,0015
39	0,2	1	0,84	26,78	26,93	0,9946	27,49	27,48	1,0005
40	0,2	1	0,76	27,93	28,12	0,9932	28,97	28,95	1,0006
41	0,2	1	0,6	30,86	31,21	0,9887	32,72	32,65	1,0022
42	0,2	1	0,44	35,37	35,85	0,9866	38,19	38,08	1,0029

Table 9: (continued): Results of GP formulation versus training results

				R_{min}		R_{min}(T/GP)	R_{max}		R_{max}(T/GP)
No:	**m**	**d/h**	**hf/h**	**Test**	**GP**		**Test**	**GP**	
43	0,2	1	0,28	45,08	45,12	0,9990	47,54	47,46	1,0017
44	0,2	1	0,2	53,71	53,86	0,9974	55,85	56,01	0,9971
45	0,3	1	0,92	25,66	25,81	0,9942	26,28	26,22	1,0020
46	0,3	1	0,76	27,59	27,84	0,9909	29,10	29,09	1,0005
47	0,3	1	0,68	28,77	29,13	0,9877	30,86	30,82	1,0013
48	0,3	1	0,6	30,13	30,67	0,9823	32,90	32,83	1,0021
49	0,3	1	0,44	35,19	35,29	0,9973	38,38	38,30	1,0023
50	0,3	1	0,28	45,10	44,99	1,0025	47,68	47,56	1,0026
51	0,3	1	0,2	53,86	53,72	1,0027	55,97	56,06	0,9984
52	0,4	1	0,92	25,57	25,73	0,9938	26,32	26,28	1,0015
53	0,4	1	0,76	27,28	27,56	0,9897	29,20	29,23	0,9990
54	0,4	1	0,68	28,30	28,73	0,9848	30,97	30,98	0,9995
55	0,4	1	0,6	30,00	30,14	0,9953	33,02	33,02	0,9999
56	0,4	1	0,52	31,83	32,02	0,9942	35,47	35,59	0,9967
57	0,4	1	0,44	34,96	35,11	0,9958	38,49	38,50	0,9998
58	0,4	1	0,36	38,91	39,15	0,9939	42,37	42,30	1,0018
59	0,4	1	0,28	44,94	44,80	1,0030	47,72	47,67	1,0011
60	0,1	2	0,92	51,99	52,01	0,9996	52,18	52,19	0,9998
61	0,1	2	0,84	54,27	54,30	0,9995	54,64	54,66	0,9997
62	0,1	2	0,76	56,91	56,95	0,9994	57,48	57,50	0,9996
63	0,1	2	0,6	63,71	63,77	0,9991	64,72	64,74	0,9997
64	0,1	2	0,52	68,23	68,32	0,9988	69,51	69,54	0,9996
65	0,1	2	0,44	73,89	74,04	0,9980	75,52	75,58	0,9992
66	0,1	2	0,28	91,93	92,09	0,9982	94,31	94,66	0,9963
67	0,1	2	0,2	108,85	108,84	1,0001	111,06	111,82	0,9932
68	0,2	2	0,92	51,87	51,89	0,9996	52,24	52,26	0,9996
69	0,2	2	0,84	54,02	54,04	0,9996	54,76	54,78	0,9996
70	0,2	2	0,76	56,53	56,54	0,9998	57,64	57,65	0,9998
71	0,2	2	0,6	62,99	63,00	0,9998	64,98	64,95	1,0005
72	0,2	2	0,52	67,23	67,29	0,9990	69,80	69,75	1,0006
73	0,2	2	0,44	72,46	72,71	0,9966	75,81	75,79	1,0003
74	0,2	2	0,28	91,51	91,37	1,0015	94,51	94,62	0,9988
75	0,2	2	0,2	108,96	108,76	1,0019	111,12	111,84	0,9936
76	0,3	2	0,92	51,74	51,76	0,9996	52,29	52,34	0,9992
77	0,3	2	0,76	56,14	56,14	1,0001	57,79	57,81	0,9996
78	0,3	2	0,68	58,92	58,91	1,0002	61,18	61,18	1,0000
79	0,3	2	0,52	66,09	66,27	0,9973	70,00	69,97	1,0003
80	0,3	2	0,36	80,61	80,00	1,0076	83,78	83,70	1,0009

81	0,3	2	0,28	91,43	91,23	1,0022	94,58	94,69	0,9988
82	0,3	2	0,2	108,61	108,62	0,9999	111,13	111,86	0,9935
83	0,4	2	0,92	51,62	51,64	0,9996	52,35	52,41	0,9987
84	0,4	2	0,84	53,52	53,53	0,9997	54,96	55,02	0,9988
85	0,4	2	0,76	55,74	55,73	1,0000	57,92	57,98	0,9991
86	0,4	2	0,68	58,32	58,33	0,9998	61,34	61,37	0,9995
87	0,4	2	0,52	66,05	65,25	1,0122	70,15	70,19	0,9995
88	0,4	2	0,44	71,83	71,80	1,0005	76,13	76,11	1,0003
89	0,4	2	0,36	79,66	79,82	0,9980	83,88	83,82	1,0007
90	0,4	2	0,28	90,53	91,04	0,9943	94,61	94,75	0,9985

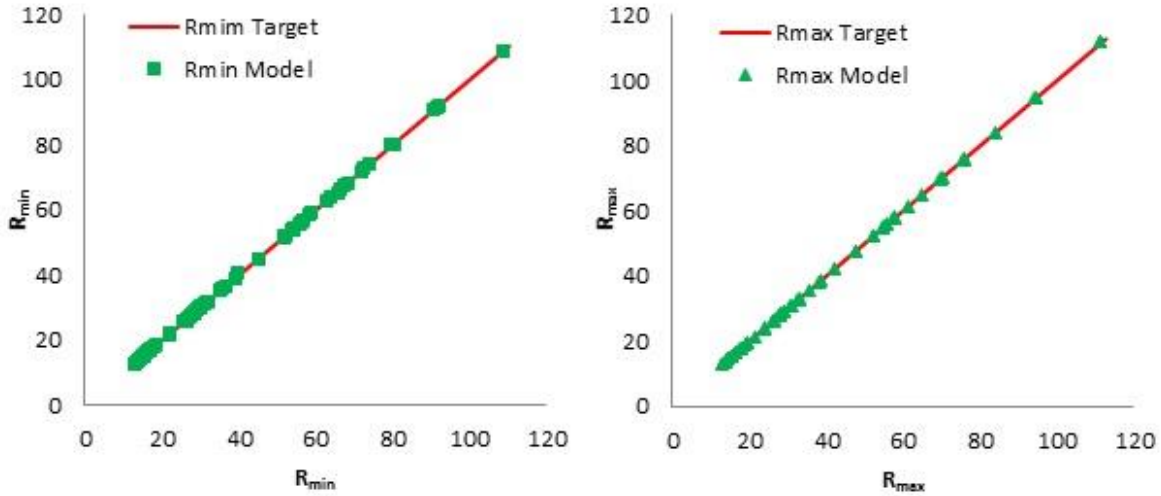

Figure 13: Training evaluation of the GEP method for the R_{min} and R_{max} prediction

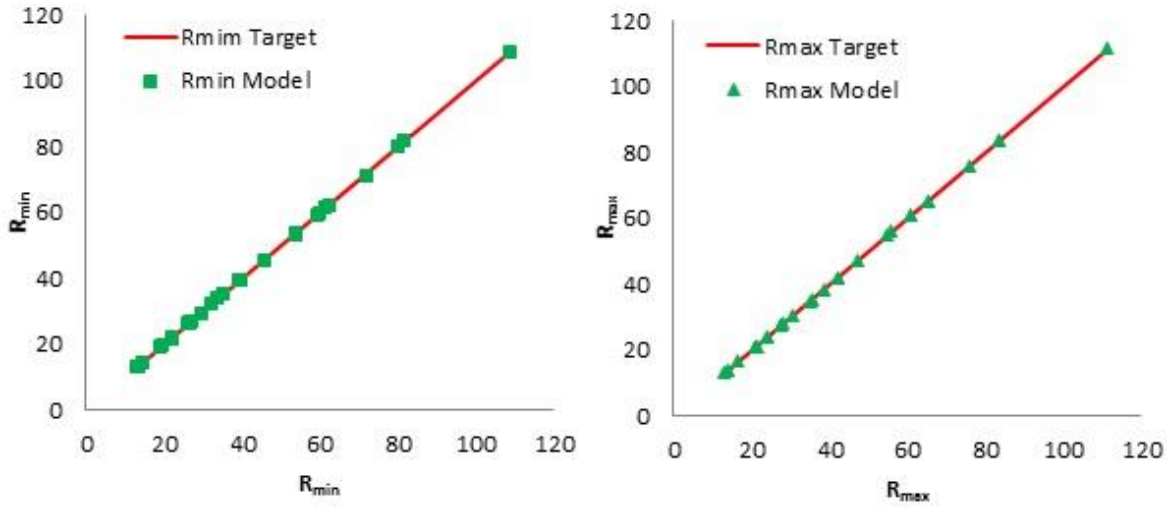

Figure 14: Test evaluation of the GEP method for the R_{min} and R_{max} prediction.

4. CONCLUSIONS

A mathematical model was generated by using GEP to predict folding point, minimum and maximum barreling radii of solid aluminum cylinders during cold upsetting. Based on the results of the present experimental study, the following conclusions have been drawn:

- A good agreement between the predicted and experimental folding point, minimum and maximum barreling radii was observed. By using the proposed GEP model, the test result of any experiment related to folding point, minimum and maximum barreling radii can be accomplished easily without doing an experiment.
- Amount of barreling and hoop strain are increasing with friction factor. Finally both ΔRmin and ΔRmax values are increasing with increasing friction factor.
- The trend of ΔRmax is very similar for different aspect ratios and they have a maximum at a specific (hf/h) value. However, ΔRmin curves are uneven after some values of (hf/h). This is due to folding where a part of the initially free surface comes into contact with the die.
- The change in radii with respect to height reduction showed different trends before and after folding processes.
- In all experiments rate of hf/h increased with the increase the friction coefficient and increase in the rate of d/h caused to decrease in the hf/h rate in all experiments.
- The performance of proposed GP models was determined as R^2= 0.908-0.998.

5. BIBLIOGRAPHY

[1] KULKARNI, M., KALPAKJIAN, S., "A study of barreling as an example of free deformation", *ASME J Eng Ind*., v.91, pp. 743-754, 1969.

[2] JOHNSON, W., MELLOR P. B., "Engineering Plasticity", *Van Nostrand Reinhold Co*., London, pp. 110-114, 1975.

[3] AVITZUR, B., "Limit analysis of disc and strip forging", *Int J Tool Des Res*., v.9, n.2, pp. 165-195, 1969.

[4] HARTLEY, P., STURGESS C. E. N., ROWE, G. W., "Friction in finite element analysis of metal forming processes", *Int. J. Mech. Sci.*, v. 21, pp. 301-306, 1979.

[5] SCHEY, A., VENNER, T. R., TAKOMA, S. L., "Shape changes in the upsetting of Slender Cylinders", *ASME J Eng Ind*, v.104, pp. 79-83, 1982.

[6] LIN, S. Y., "An Investigation of Un equal interface frictional conditions during the upsetting process", *J Mater Proc. Tech.*, v.65, pp. 292,301, 1997.

[7] YANG, D. Y., CHOI, Y., KIM, J. H., "Analysis of upset forging of cylindrical billets considering the dissimilar frictional conditions at two flat die surfaces", *Int J. Mach. Tool Manuf.*, v. 4, pp. 44-50, 2004.

[8] KOBAYASHI, S., AND OH, S. I., "Fracture criterion for materials in plastic deformation processes", *Tech Report AFML-TR-74-159*, 1974.

[9] SALUJA, S. S., PANDEY, P. C., DALELA, S., "A simple method for flow stress determination under metal working conditions", *9th NAMRC*, pp. 153-157, 1981.

[10] MALAYAPPAN S., ESAKKIMUTHU, G., "Barreling of Aluminum solid cylinders during cold upsetting with different frictional conditions at the faces", *Int. J. Adv. Manuf. Technol.*, v. 29, pp. 41-48, 2006.

[11] BASKARAN, K., NARAYANASAMY, R., "Some aspects of barreling in elliptical shaped billets of aluminum during cold upset forging with lubricant", *Materials and Design*, v. 29, pp. 638-661, 2008.

[12] LAHOTI, G. D., NAGPAL, V., ALTAN, T., "Numerical Method for Simultaneous Prediction of Metal Flow and Temperatures in Upset Forging of Rings", *Trans ASME J Eng Ind*, v.100, n.4, pp. 413-420, 1978.

[13] KOZA J.R., *Genetic Programming: On the Programming of Computers by Means of Natural Selection*, Cambridge (MA), MIT press, 1992.

[14] DAVIDSON J. V., SAVIC D. A., WALTERS G.A., "Symbolic and numerical regression: Experiments and application", *Information Sciences*, v.150, n.1/2, pp. 95-117, 2003.

[15] ONG C. S., HUANG J. J., TZENG G. H., "Building credit scoring models using genetic programming", *Expert Systems with Applications*, v.29, n.1, pp 41-47, 2005.

[16] ASBOUR, A. F, ALVAREZ L. F, TOROPOV V.V., ''Emprical modeling of shear strength of rc deep beams by genetic programming'', *Computers and Structures*, v. 81, n. 5, pp. 331-338, 2003.

[17] FERREIRA C., *Gene expression programming: mathematical modelling by an artificial intelligence*, 2nd Edition, Springer, 2006.

[18] ESKIL, M., KANCA, E., "A new formulation for martensite start temperature of Fe–Mn–Sishape memory alloys using genetic programming", *Computational Materials Science*, v.43, pp. 774–784, 2008.

[19] THAHEER, A. S. A., NARAYANASAMY, R. "Comparison of barreling in lubricated truncated cone billets during cold upset forging of various metals", *Materials and Design*, v.29, pp.1027–1035, 2008.

[20] MANISEKAR K., and NARAYANASAMY R. "Effect of friction on barrelling in square and rectangular billets of Aluminium during cold upset forging", *Materials and Design*, v. 28, pp. 592–598, 2007.

ORCID

Erdoğan Kanca https://orcid.org/0000-0002-7997-9631
Ömer Eğercioğlu https://orcid.org/0000-0002-9076-0972
Ali Günen https://orcid.org/0000-0002-4101-9520
Mehmet Demir https://orcid.org/0000-0001-8372-5856